Research Article

Weiyi Ma, Yi Jiang*, Han Zhang, Liuchao Zhang, Jie Hu, and Lan Jiang

Miniature on-fiber extrinsic Fabry-Perot interferometric vibration sensors based on micro-cantilever beam

https://doi.org/10.1515/ntrev-2019-0028
Received Jun 26, 2019; accepted Aug 27, 2019

Abstract: An on-fiber extrinsic Fabry–Perot interferometric (EFPI) vibration sensor based on micro-cantilever beam is proposed and experimentally demonstrated. The micro-cantilever beam, with a cantilever length of 80μm and a cantilever thickness of 5μm, is created perpendicular to the fiber axis by using the femtosecond laser micromachining technique. The on-fiber vibration sensor has same diameter with that of the single mode fiber. An acceleration sensitivity of 11.1 mV/g@300 Hz in the range of 0.5-5g is demonstrated experimentally. This on-fiber and micro-cantilever beam design allows for the sensor to be smaller size and higher temperature resistance.

Keywords: Extrinsic Fabry–Perot interferometer; vibration sensor; fiber optical sensor; femtosecond laser micromachining

1 Introduction

Vibration sensors have found wide applications in many areas such as in structural health monitoring [1], inertial navigation [2], earthquake monitoring [3] and even biomedicine [4]. Some of these applications, like endoscopic photoacoustic imaging [5] and turbine engines [6], require vibration sensors with small size, high sensitivity, biocompatible structure and high temperature resistance. However, most of commercially available vibration sensors (capacitive [7] or piezoelectric [8] based vibration transducers) suffer from oversize, electromagnetic interference and high temperature softening, which make them difficult for vibration measurements in such a harsh environment. In this case, optical fiber vibration sensors offer a potential solution as they possess many advantages over the conventional electrical vibration sensors such as being passive, small size, immunity to electromagnetic interference and amiability to high temperature conditions [9, 10].

Various types of optical fiber vibration sensors have been demonstrated. Early intensity-based optical fiber vibration sensors employ low cost and not very sophisticated instrumentation [11]. The main disadvantages of these vibration sensors are their low precision and stability. Fiber Bragg grating (FBG)-based vibration sensors are considered to have good sensitivity and unique multiplexing capability [10, 12, 13]. However, their sensor dimensions and the instability under high temperature have limited their applications. Fabry–Pérot interferometer (FPI)-based vibration sensors have played a dominant role due to their capacity for miniature size and high stability [14–19]. These vibration sensors typically utilize a sensor head that carries an extrinsic Fabry–Pérot interferometric (EFPI) structure and a cantilever beam or support beam. In most cases, the dimension of the sensor head is larger than the optical fiber diameter and the applications of bonding materials (polymeric adhesives) may yield low tensile-strength structures. Consequently, the vibration range and long-term stability of these sensors are limited. By using the all-fiber sensor design, it is possible to reduce the vibration sensor diameter down to the Ø 125μm range [16, 17, 19]. Moreover, sensors with all-fiber structure proved to be robust and temperature and otherwise environmentally stable. The main obstacle is to operate on the fiber to fabricate a desired sensing structure. Chemical etching method has simple manufacturing steps and low costs [16]. However, due to the limited precision of the etching process, the sensor dimension is typically a few hundred micrometers. Two strategies have been followed to overcome the problem. The first is to employ focused ion beam (FIB) processing technique. With the combination of FIB technology

***Corresponding Author: Yi Jiang:** School of Optics and Photonics, Beijing Institute of Technology, Beijing, 100081, China; Email: bitjy@bit.edu.cn
Weiyi Ma, Liuchao Zhang: School of Optics and Photonics, Beijing Institute of Technology, Beijing, 100081, China
Han Zhang: Key Laboratory of Noise and Vibration, Institute of Acoustics, CAS, Beijing, 100190, China
Jie Hu, Lan Jiang: Laser Micro/Nano Fabrication Laboratory, School of Mechanical Engineering, Beijing Institute of Technology, Beijing, 100081, China

and hydrofluoric acid etching, the cantilever structure has achieved a dozen micrometers diameter and high sensitivity to applied vibrations [17]. Two associated drawbacks of the FIB processing technique however are the costly equipment and the time it takes to machine the cantilever structure. The second and more appropriate approach towards an all-fiber solution is to use a femtosecond laser (FSL). While the FSL micromachining technique is not as accurate as the FIB processing technique, it shows higher efficiency and lower costs [19].

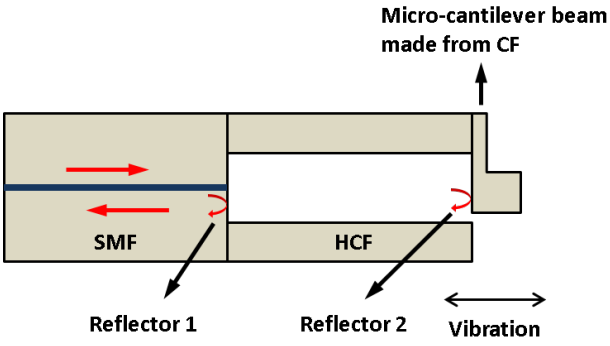

Figure 1: Schematic of the proposed on-fiber EFPI vibration sensor

In this paper, we present an on-fiber EFPI vibration sensor with a micro-cantilever beam fabricated by a femtosecond laser. The micro-cantilever beam is created perpendicular to the fiber axis, which makes the cantilever length less than the diameter of single mode fiber. All the processing steps are straightforward and easy to operate.

2 Sensor design and fabrication

2.1 Design of the sensor structure

The designed vibration sensor consists of a standard lead-in single mode fiber (SMF), a hollow core fiber (HCF) and a micro-machined silica coreless fiber (CF), as shown in Figure 1. The end face of the SMF and the back surface of the CF form a Fabry–Perot (FP) cavity. The CF is processed into a micro-cantilever beam integrating with an inertial mass for vibration detecting. Under applied vibration acting on the sensor, the micro-cantilever beam deflects due to inertia and the inertial mass from the beam oscillates along the axial direction, resulting in a change in the cavity length correspondingly. Thus, the vibration can be detected by using the quadrature operating-point demodulation.

2.2 Fabrication procedure of the sensor

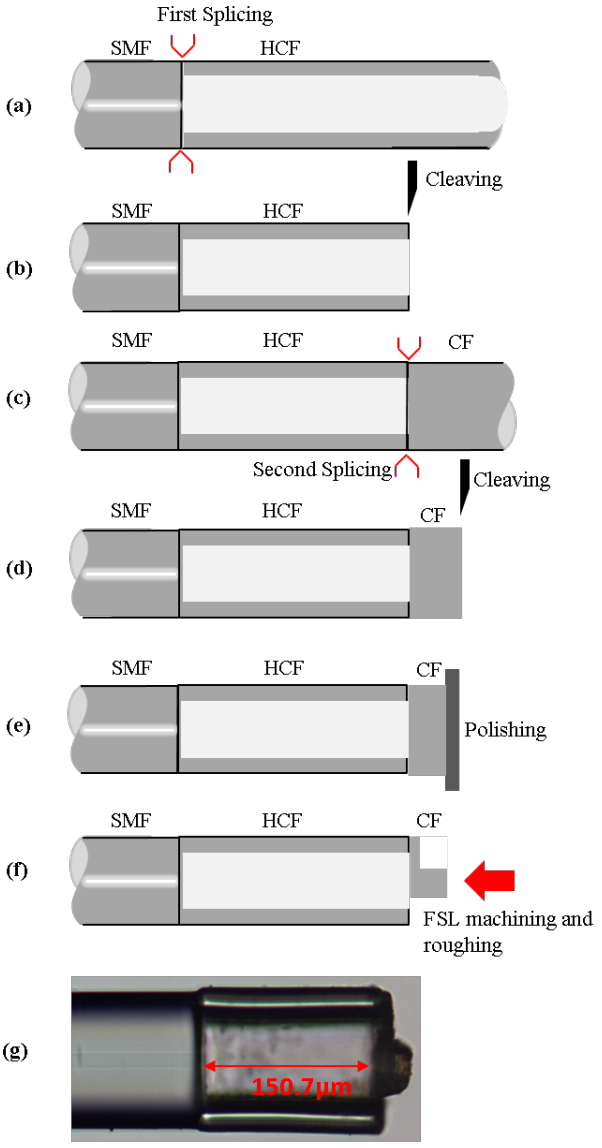

Figure 2: Fabrication procedure for the vibration sensor (a)–(f) and an optical microscope picture of a fabricated sensor (g)

Sensor fabrication consists of a sequence of steps which are shown in Figure 2. After a SMF (SMF-28e, Corning) and a HCF were cleaned and polished, the first splice between the SMF and the HCF was achieved by use of a commercial fiber splicer. The inner and outer diameter of the HCF is 93μm and 130μm respectively [Figure 2(a)]. Then the HCF was cleaved to a specified length (∼ 150μm) using a fiber cleaver under the assistance of an optical microscope [Figure 2(b)]. Next, the second splice was performed by splicing this sample to a coreless silica fiber (CF)

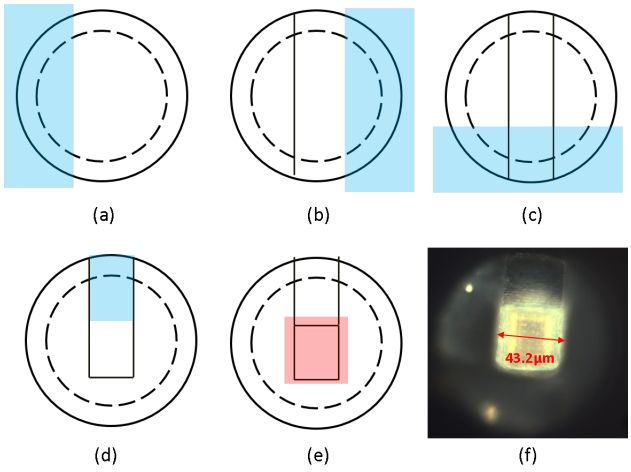

Figure 3: Micromachining procedures for micro-cantilever beam structure (a)–(e) and an optical microscope picture of the end face of a fabricated sensor (f)

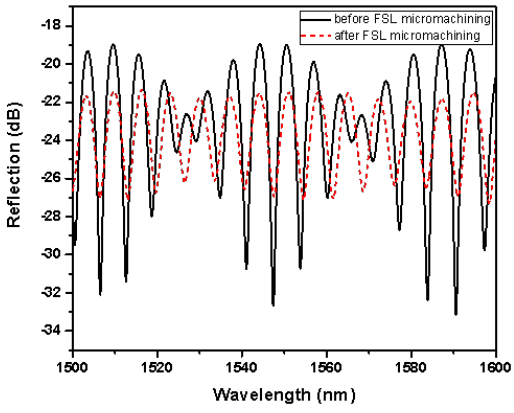

Figure 4: Interference spectrums before and after the FSL micromachining

[Figure 2(c)]. This was followed by cutting the CF ~50μm away from the spliced location [Figure 2(d)]. Afterwards, the CF was further polished to the needed length (30μm) to form a thin diaphragm [Figure 2(e)]. Finally, the SMF-HCF-CF sandwich structure was fixed on a hexapod six-axis stage and machined into a desired micro-cantilever beam structure by using the FSL [Figure 2(f)]. Figure 2(g) is an optical microscope picture of the side view of a typical vibration sensor fabricated by this method.

The micromachining procedures of the micro-cantilever beam structure was schematically described in Figure 3. The FSL (5 W, Spectra-Physics) with a central wavelength of 800 nm, a repetition rate of 1 kHz, a pulse width of 35 fs, and a pulse energy of 40 μJ was focused onto the outside surface of the CF (*i.e.*, the diaphragm) by employing an objective lens (MPlan FL N, Olympus). Then a part of the CF was ablated to form a preliminary cantilever structure [Figure 3(a) - Figure 3(c)]. This structure had a length of about 80μm and a width of 45μm. Since the whole ablation region of the CF had to be cleaved until the hole of the HCF exposed, the preliminary thickness of the cantilever was equal to the thickness of diaphragm (30μm). Next, the preliminary cantilever was further trimmed in order to obtain a vibration -sensitive micro-cantilever beam structure. This was performed by thinning the upper part of the cantilever to an optimal dimension [Figure 3(d)], which determined the vibration sensitivity of the sensor. While the selection of a thinner cantilever would be feasible, the thinner cantilever might be frail and easy to crack. In this paper, the thickness of the cantilever was determined to be 5μm. After the updated micro-cantilever was machined, the undressed section can serve as the inertial mass. In Figure 3(e), the inertial mass was roughened to suppress unwanted back-reflections from its outer surface. Figure 3(f) shows the cross section of the machined micro-cantilever beam used in the experiment.

During CF polishing [Figure 2(e)], the precise control over the CF thickness is achieved by connecting the sample to a homemade white-light interferometric (WLI) interrogator system (0.2 nm resolution and 1 Hz measurement frequency). The white-light interference spectrum was continuously obtained by the interrogator and the thickness of the CF can be calculated in real time. Figure 4 shows the interference spectrum of the representative sample whose CF thickness has been polished down to 30μm. The black line, which was obtained before the FSL micromachining, was the contribution of three reflectors, one from the end face of the SMF and the other two from both inner and outer surface of the CF. The three-beam interference is viewed as the superposition of two-beam interferences which can be interrogated (calculating the CF thickness) by using the FFT-based WLI and peak to peak method, as described in detail in our previous publication [20–22]. The red dashed curve was obtained after the inertial mass roughening [Figure 3(e)]. Note that the reflection from the outer surface of inertial mass has been suppressed and the two-beam interference with a fringe contrast of 5dB is formed.

3 Experiments and evaluations

3.1 Experimental setup

To obtain the vibration signal of the sensor, the quadrature operating-point demodulation technique is adopted by de-

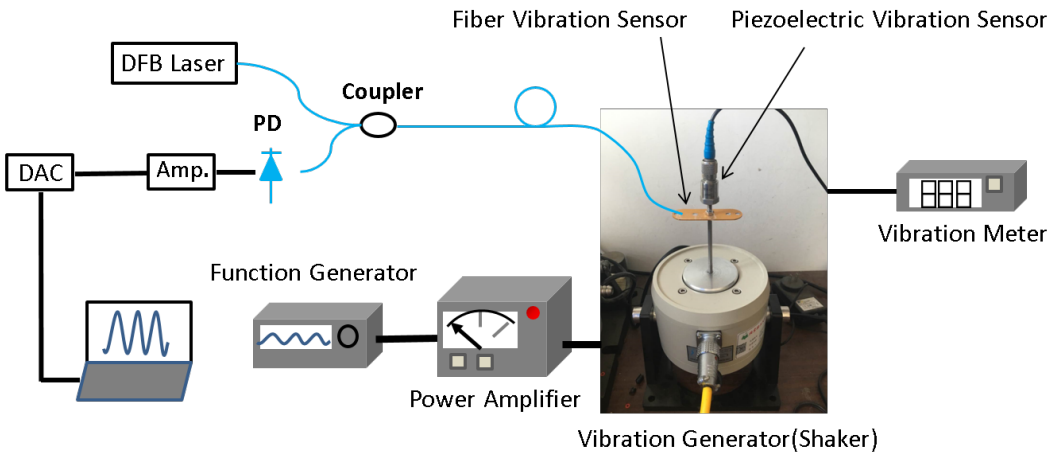

Figure 5: Experimental setup for vibration sensor evaluation

tecting the variation of operating point wavelength. When the incident light from the SMF is reflected at two fiber/air interfaces, a sinusoidal interference signal from the EFPI is formed. Typically, the operating point is chosen in the linear region of the sinusoidal interference signal to achieve a linear response with high sensitivity. In case of applied vibration, the variation in the operating point wavelength due to a change of the air cavity length provides the desired intensity variation of output voltages. This intensity variation is proportional to the applied vibration and can be used for vibration or acceleration detecting. The variation in the operating point wavelength can be described as: $\Delta\lambda_l = \lambda_l \cdot \Delta L/L$, where λ_l is the operating point wavelength, ΔL is the change of the air cavity length and $L$is the air cavity length [23].

The experimental setup for vibration tests is schematically shown in Figure 5. A distributed feedback (DFB) laser was used as the light source, whose center wavelength was 1550.02 nm. Light from the laser was launched into the vibration sensor through a coupler and the reflected light was detected by a photodetector (PD), followed by an amplifier circuit (Amp.). A data acquisition card (DAC) with a sampling frequency of 15 kHz was employed to sample the signal. The vibration sensor was fixed on a shaker (JSK-5T, Jiangsu Lianneng, China) where the cantilever beam was perpendicular to the vibration direction. A function generator and a power amplifier were connected to the shaker for signal generating and driving. When the shaker was excited and oscillated along the fiber axial direction, the applied vibration signal was sampled and processed. During oscillating, a piezoelectric vibration sensor (YD84T, Amphenol) was placed where the fiber sensor was to be tested for calibration purpose facilitated by a vibration meter (VT-63, Shanghai Wujiu, China).

3.2 Time response and frequency response of the sensor

Figure 6 demonstrates the time response and related frequency response of the vibration sensor when an external oscillation with a frequency of 300 Hz and an acceleration of 2.5 g is applied to the shaker. The frequency spectrum of the sensor [Figure 6(b)] is given by the fast Fourier transform (FFT). It is seen that the FFT spectra has a signal-to-noise ratio (SNR) of 33 dB and the measured frequency is in agreement with the applied frequency. This coincidence can also be demonstrated from the vibrational spectrum of sensor [Figure 6(a)] whose amplitude would be used for acceleration measurements.

3.3 Acceleration response of the vibration sensor

Figure 7 shows the acceleration response of the vibration sensor versus the external oscillation. The frequency was adjusted to 300 Hz and the applied acceleration was determined by the vibration meter. Since the tip displacement of a cantilever-mass architecture is proportional to the acceleration, the amplitude of the vibrational spectrum can be considered as the result of the acceleration response. The applied acceleration began at 0.5g (almost 9.8 m/s^2) and increased incrementally to 5 g in steps of 0.5 g. Each measurement was repeated five times and the mean value was recorded. As expected, the response amplitude shows good linearity with the applied acceleration, with a correlation coefficient (R) of 0.99078. The response sensitivity of sensor is estimated to be 11.1mV/g by calculating the slope of the linear fitting curve.

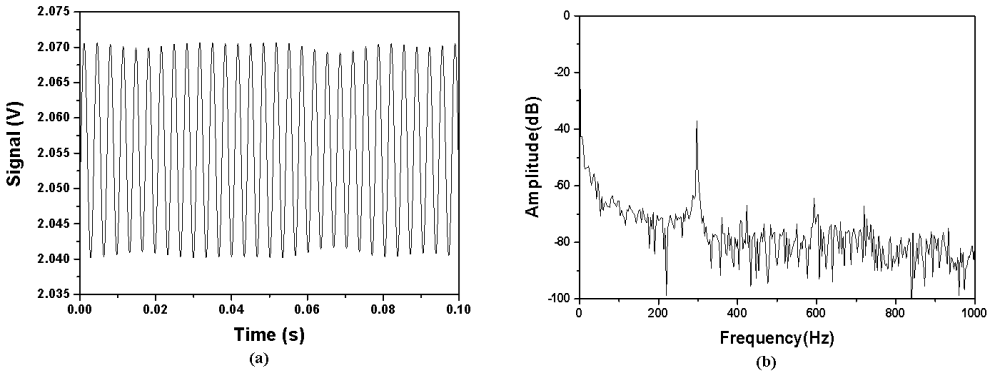

Figure 6: The demodulated vibration signals (a) and its FFT spectra (b) under the applied vibration frequency of 300 Hz and the acceleration of 2.5 g.

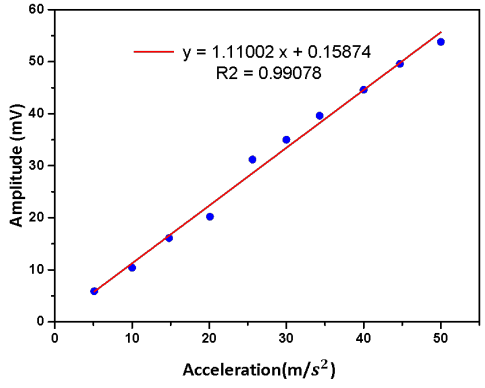

Figure 7: The acceleration response of the vibration sensor.

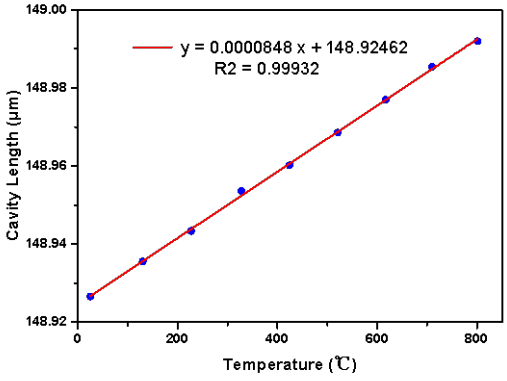

Figure 8: The relationship between the cavity length and the applied temperature.

The temperature dependence of the vibration sensor was further investigated. The homemade WLI interrogator system was used to obtain the cavity length of the EFPI in different temperatures. The temperature dependence, which is attributed to the thermal expansion effect of the HCF, can be expressed as $\Delta L = L_0 \cdot \alpha \cdot \Delta T$, where $\alpha$is the coefficient of thermal expansion of silica ($0.55 \times 10^{-6}/°C$), L_0 is the initial cavity length (150μm), ΔL and ΔT are the change of the EFPI cavity length and applied temperature respectively. Thus, the predicted temperature sensitivity of the sensor is calculated to be $\Delta L/\Delta T$ = 0.083nm/°C. Figure 8 shows experimental results of the cavity length as a function of applied temperature. Note that the measured EFPI cavity length has a good linear correlation to the applied temperature and the temperature sensitivity is obtained to be 0.0848 nm/°C, which is in reasonable agreement with the predicted value of 0.083nm/°C. In addition, the obtained temperature sensitivity indicate that fluctuations of $\sim$ 800°C (the temperature measurement range) would induce a cavity length error of $\Delta L \approx$ 67.84nm, resulting in a variation in the operating point wavelength of $\Delta\lambda_l \approx$ 0.7nm ($\lambda_l \approx$ 1550nm). Such a shift is very low compared to the FSR of the interference spectrum in Figure 4 and the temperature compensation would not be necessary.

4 Conclusion

In conclusion, an on-fiber vibration sensor with a dimension as small as the standard fiber diameter (125μm) has been proposed and experimentally demonstrated. The vibration sensor is composed of a standard lead-in SMF, a HCF and a micro-machined CF, which has a micro-cantilever beam structure. The micro-cantilever beam is created perpendicular to the fiber axis, which makes the cantilever length (80μm) less than the standard fiber diam-

eter. The end face of the SMF and the back surface of the micro-cantilever beam form an EFPI cavity. A representative sensor with an acceleration sensitivity of 11.1mV/g was fabricated and tested. This on-fiber and cross-axial micro-cantilever beam designs render the sensor smaller size and higher temperature resistance.

Acknowledgement: This work was supported in part by the National Key R&D Program of China under Grant 2018YFB1107200, the National Natural Science Foundation of China (NSFC) under Grants 61775020 and 61575021.

Conflict of Interests: The authors declare no competing financial interests regarding the publication of this paper.

References

[1] Strasberg M., Feit D., Vibration damping of large structures induced by attached small resonant structures, J. Acoust. Soc. Amer., 1996, 99, 335-344.

[2] Tan C.W., Park S., Design of accelerometer-based inertial navigation systems, Ieee T. Instrum. Meas., 2005, 54, 2520-2530.

[3] Bertolini A., DeSalvo R., Fidecaro F., Francesconi M., Marka S., Sannibale V., Simonetti D., Takamori A., Tariq H., Mechanical design of a single-axis monolithic accelerometer for advanced seismic attenuation systems, Nucl. Instrum. Meth. A., 2006, 556, 616-623.

[4] Ashkenazi S., Hou Y., Buma T., O'Donnell M., Optoacoustic imaging using thin polymer etalon, Appl. Phys. Lett., 2005, 86.

[5] Zhang E.Z., Beard P.C., A miniature all-optical photoacoustic imaging probe, Photons Plus Ultrasound: Imaging And Sensing, 2011, 2011, 7899.

[6] Maynard K., Trethewey M., Gill R., Resor B., Gas turbine blade and disk crack detection using torsional vibration monitoring: A feasibility study, Cond. Monitor. Diagn. Eng. Manag., 2001, 985-992.

[7] Kulah H., Chae J., Naiari K., Noise analysis and characterization of a sigma-delta capacitive silicon microaccelerometer, Boston Transducers'03: Digest of Technical Papers, 2003, 1,2, 95-98.

[8] Tadigadapa S., Mateti K., Piezoelectric MEMS sensors: state-of-the-art and perspectives, Meas. Sci. Technol., 2009, 20(9), 092001.

[9] Lee B., Review of the present status of optical fiber sensors, Opt. Fiber Technol., 2003, 9, 57-79.

[10] Tsuda H., Fiber Bragg grating vibration-sensing system, insensitive to Bragg wavelength and employing fiber ring laser, Opt. Lett., 2010, 35, 2349-2351.

[11] Kalenik J., Pajak, A cantilever optical-fiber accelerometer, Sensor Actuat. a-Phys., 1998, 68, 350-355.

[12] Basumallick N., Chatterjee I., Biswas P., Dasgupta K., Bandyopadhyay S., Fiber Bragg grating accelerometer with enhanced sensitivity, Sensor Actuat. a-Phys., 2012, 173, 108-115.

[13] Guo T., Ivanov A., Chen C.K., Albert J., Temperature-independent tilted fiber grating vibration sensor based on cladding-core recoupling, Opt. Lett., 2008, 33, 1004-1006.

[14] Ke T., Zhu T., Rao Y.J., Deng M., Accelerometer Based on All-Fiber Fabry-Perot Interferometer Formed by Hollow-Core Photonic Crystal Fiber, Microw. Opt. Techn. Let., 2010, 52, 2531-2535.

[15] Jia P.G., Wang D.H., Yuan G., Jiang X.Y., An Active Temperature Compensated Fiber-Optic Fabry-Perot Accelerometer System for Simultaneous Measurement of Vibration and Temperature, IEEE Sens. J., 2013, 13, 2334-2340.

[16] Zhang Q., Zhu T., Hou Y.S., Chiang K.S., All-fiber vibration sensor based on a Fabry-Perot interferometer and a microstructure beam, J. Opt. Soc. Am. B., 2013, 30, 1211-1215.

[17] Andre R.M., Pevec S., Becker M., Dellith J., Rothhardt M., Marques M.B., Donlagic D., Bartelt H., Frazao O., Focused ion beam post-processing of optical fiber Fabry-Perot cavities for sensing applications, Opt. Express, 2014, 22, 13102-13108 .

[18] Li J., Wang G.Y., Sun J.N., Maier R.R.J., Macpherson W.N., Hand D.P., Dong F.Z., Micro-Machined Optical Fiber Side-Cantilevers for Acceleration Measurement, Ieee Photonic Tech. L., 2017, 29, 1836-1839.

[19] Zhang L.C., Jiang Y., Jia J.S., Wang P., Wang S.M., Jiang L., Fiber-optic micro vibration sensors fabricated by a femtosecond laser, Opt. Laser Eng., 2018, 110, 207-210.

[20] Jiang Y., Fourier transform white-light interferometry for the measurement of fiber-optic extrinsic Fabry-Perot interferometric sensors, IEEE Photonic Tech. L., 2008, 20, 75-77.

[21] Jiang Y., High-resolution interrogation technique for fiber optic extrinsic Fabry-Perot interferometric sensors by the peak-to-peak method, Appl. Optics, 2008, 47, 925-932 .

[22] Gao H.C., Jiang Y., Cui Y., Zhang L. C., Jia J.S., Hu J., Dual-Cavity Fabry-Perot Interferometric Sensors for the Simultaneous Measurement of High Temperature and High Pressure, IEEE Sens. J., 2018, 18, 10028-10033.

[23] Bremer K., Lewis E., Leen G., Moss B., Lochmann S., Mueller I.A.R., Feedback Stabilized Interrogation Technique for EFPI/FBG Hybrid Fiber-Optic Pressure and Temperature Sensors, IEEE Sens. J., 2012, 12, 133-138.